# The Differential Palmitoylation States of N-Ras and H-Ras Determine Their Distinct Golgi Sub-compartment Localizations

**ARTICLE** *in* JOURNAL OF CELLULAR PHYSIOLOGY · MARCH 2015

Impact Factor: 3.84 · DOI: 10.1002/jcp.24779



**6 AUTHORS**, INCLUDING:

Mark R Philips
NYU Langone Medical Center
**105** PUBLICATIONS **7,780** CITATIONS
SEE PROFILE

Angel Pellicer
NYU Langone Medical Center
**149** PUBLICATIONS **11,616** CITATIONS
SEE PROFILE

Journal of Cellular Physiology



# The Differential Palmitoylation States of N-Ras and H-Ras Determine Their Distinct Golgi Subcompartment Localizations

STEPHEN J. LYNCH,[1] HARRIET SNITKIN,[2] IWONA GUMPER,[2] MARK R. PHILIPS,[2,3,4,5] DAVID SABATINI,[2] AND ANGEL PELLICER[1,5]*

[1]*Department of Pathology, New York University School of Medicine, New York, New York*

[2]*Department of Cell Biology, New York University School of Medicine, New York, New York*

[3]*Department of Medicine, New York University School of Medicine, New York, New York*

[4]*Department of Pharmacology, New York University School of Medicine, New York, New York*

[5]*New York University Cancer Institute, New York University School of Medicine, New York, New York*

Despite a high degree of structural homology and shared exchange factors, effectors and GTPase activating proteins, a large body of evidence suggests functional heterogeneity among Ras isoforms. One aspect of Ras biology that may explain this heterogeneity is the differential subcellular localizations driven by the C-terminal hypervariable regions of Ras proteins. Spatial heterogeneity has been documented at the level of organelles: palmitoylated Ras isoforms (H-Ras and N-Ras) localize on the Golgi apparatus whereas K-Ras4B does not. We tested the hypothesis that spatial heterogeneity also exists at the sub-organelle level by studying the localization of differentially palmitoylated Ras isoforms within the Golgi apparatus. Using confocal, live-cell fluorescent imaging and immunogold electron microscopy we found that, whereas the doubly palmitoylated H-Ras is distributed throughout the Golgi stacks, the singly palmitoylated N-Ras is polarized with a relative paucity of expression on the *trans* Golgi. Using palmitoylation mutants, we show that the different sub-Golgi distributions of the Ras proteins are a consequence of their differential degree of palmitoylation. Thus, the acylation state of Ras proteins controls not only their distribution between the Golgi apparatus and the plasma membrane, but also their distribution within the Golgi stacks.

J. Cell. Physiol. 230: 610–619, 2015. 

There are three Ras genes in mammals: *nras*, *hras,* and *kras*. Through alternative splicing of exon 4, the *kras* gene gives rise to two isoforms: K-Ras4A and K-Ras4B (Ahearn et al., 2011a). The observations that the Ras proteins share a high degree of structural similarity and that the *hras*, *kras,* and *nras* oncogenes are interchangeable in their ability to induce cellular transformation in vitro led to the proposal that the Ras isoforms are functionally redundant (Barbacid, 1987; Castellano and Santos, 2011). However, it is now clear that the Ras proteins play distinct cellular functions, which is a reflection of significant sequence divergence that is localized exclusively to their 24–25 amino acid C-terminal regions, known as the hyper-variable region (HVR). In the case of N-Ras, H-Ras, and K-Ras4A, the HVR contains sites for post-translational farnesylation and for the addition of one (in N-Ras and K-Ras4A) or two (in H-Ras) palmitoyl moieties. The addition of farnesyl and palmitoyl groups to the C-terminal regions of N-Ras, H-Ras, and K-Ras4A, which occurs sequentially, is required for both their membrane association and for their translocation from the Golgi apparatus to the plasma membrane (PM), which are, in turn, important for the regulation of Ras activity by PM-localized guanine nucleotide exchange factors and GTPase-activating proteins (Ahearn et al., 2011a). Ras proteins that have been farnesylated and palmitoylated have a one hundred-fold higher affinity for membranes than Ras proteins that have only been farnesylated (Ahearn et al., 2011a). Palmitoylation, therefore, has the effect of "affinity trapping" Ras in Golgi membranes and thereby promoting their translocation to the PM through the vesicular transport pathway. K-Ras4B is farnesylated, but not palmitoylated, and the second signal required for membrane association of K-RasB is a highly positively charged, lysine-rich region localized to its HVR.

The palmitoyl acyltransferase (PAT) responsible for palmitoylation of Ras has been identified as DHHC9-GCP16 (DHHC domain-containing 9-Golgi complex-associated protein of 16 kDa), a heterodimeric protein complex consisting of two multiple-membrane spanning proteins with the active site disposed toward the cytosolic face of the Golgi membranes (Swarthout et al., 2005). Palmitoylation is a reversible modification and Ras proteins have been shown to undergo a cycle of palmitoylation and depalmitoylation, which promotes their anterograde and retrograde transport, respectively, between the Golgi apparatus and the PM (Goodwin et al., 2005; Rocks et al., 2005). Activated Ras proteins can signal not only from the PM but from endomembrane compartments, including Golgi membranes (Chiu et al., 2002; Perez de Castro et al., 2004), and it has been proposed that regulation of the Ras palmitoylation-depalmitolyation cycle can be a means to control compartmentalized Ras signaling (Lorentzen et al., 2010). An enzyme with clear-cut Ras deacylating activity has

Contract grant sponsor: NIH;
Contract grant numbers: GM055279, CA118495.
Contract grant sponsor: Leukemia and Lymphoma Society;
Contract grant number: LLS6099–12.

*Correspondence to: Angel Pellicer, New York University School of Medicine, Department of Pathology, 550 First Avenue, MSB 563, New York 10016, NY.
E-mail: angel.pellicer@nyumc.org

Manuscript Received: 22 July 2014
Manuscript Accepted: 22 August 2014

Accepted manuscript online in Wiley Online Library (wileyonlinelibrary.com): 27 August 2014.
DOI: 10.1002/jcp.24779

not yet been identified. The acyl protein thioesterase APT1 has been implicated in Ras protein deacylation (Dekker et al., 2010), however, its localization in the cytosol and substrate promiscuity preclude a definitive assignment. We have previously shown that the prolyl isomerase, FKB12 (FK506 binding protein 12) binds to palmitoylated Ras and promotes its deacylation through *cis-trans* isomerization of a N-terminal peptidyl-prolyl bond (Ahearn et al., 2011b). The thioester linkage between palmitate and its substrates is quite labile, and it has also been proposed that deacylation of the Ras proteins might be non-enzymatic (Ahearn et al., 2011a).

Despite initial claims that the Ras proteins are functionally redundant, more recent work has provided evidence for functional specificity of the Ras isoforms (Castellano and Santos, 2011). Our group (Leon et al., 1987) showed that different *ras* mRNAs are expressed in a tissue-specific manner with different temporal dynamics. Additionally, disruption of the *kras* gene in mice results in embryonic lethality (Koera et al., 1997), whereas mice with disruption of *nras, hras,* or both *nras* and *hras* have no developmental phenotype (Umanoff et al., 1995; Esteban et al., 2001). Although the results from these studies imply that *nras* and *hras* (but not *kras*) are dispensable during development, the observation that *hras* can functionally substitute for *kras* when cloned into the *kras* locus (Potenza et al., 2005) suggests instead that different spatio-temporal patterns of Ras expression rather than differences in the biological activity of different Ras proteins is the primary determinant of functional specificity of the ras genes. Another compelling indication of functional heterogeneity is the differential association of oncogenic Ras isoforms with specific human tumors. Pancreatic adenocarcinoma is almost always associated with an activating mutation of *kras* whereas melanomas are often associated with *nras* mutations (Bos, 1989). Finally, different Ras isoforms have been found to be organized in distinct PM nanoclusters that function as nucleation centers for downstream signaling (Parton and Hancock, 2004; Plowman and Hancock, 2005; Roy et al., 2005).

Accumulating evidence has implicated N-Ras as the isoform that plays the most prominent role in the development of the hematopoietic system. Studies by our group (Leon et al., 1987) found that *nras* mRNA is preferentially expressed in the thymus, implying that N-Ras plays a role in the development of cells in this organ. Studies of patient populations have shown that oncogenic N-Ras mutations are associated with the development of hematopoietic cancers, including acute myeloid leukemia (AML) and myelodysplastic syndrome (Farr et al., 1988; Jannsen et al., 1987). In addition, over-expression of oncogenic N-Ras in mice was associated with a high incidence of hematopoietic malignancies (Mangues and Pellicer, 1992; Parikh et al., 2006). Although initial work showed that *nras* KO mice did not exhibit an obvious phenotype (Umanoff et al., 1995), further studies by our group revealed that a subtle immune cell-specific phenotype was associated with the absence of *nras* (Perez de Castro et al., 2003). Decreases in the size of single positive T-cell populations were observed in *nras* knockout mice, implying defects in the process of positive selection. Most strikingly, *nras* KO mice were also unable to respond to an influenza challenge.

A follow up study (Perez de Castro et al., 2004) provided a mechanistic explanation for the preferential role played by N-Ras in immune cell development and function. When Jurkat T-cells were treated with a low-level T-cell receptor (TCR) stimulus, N-Ras was preferentially activated on Golgi membranes, but not at the PM. It has been shown that Ras proteins could be activated at and signal from intracellular membranes (Chiu et al., 2002) and further studies provided the first indication for specific N-Ras isoform activation at intracellular membranes in immune cells (Perez de Castro et al., 2004). This work also highlighted the importance of the palmitoylation state of the Ras isoform in the specificity of Ras signaling from the Golgi membrane. Thus, in Jurkat cells, a mono-palmitoylated H-Ras mutant (H-RasC184L, a.k.a. H-Ras-Palm*N*) could be activated at and signal from Golgi membranes after a low-level TCR stimulus. Conversely, a doubly-palmitoylated N-Ras mutant (N-RasL184C, a.k.a. N-Ras-Palm*H*) could neither be activated at, nor signal from Golgi membranes (Perez de Castro et al., 2004). These results supported the hypothesis that the palmitoylation state of the Ras isoform determines its capacity to be functionally activated at Golgi membranes of T-cells.

In the present study, utilizing confocal live-cell imaging and immuno-EM, we show that N-Ras and H-Ras have distinct patterns of Golgi membrane localization, which are determined by the palmitoylation state of the Ras isoforms.

## Results

### Confocal live-cell imaging reveals distinct patterns of N-Ras and H-Ras localization within Golgi cisternal membranes

To establish the localization of N-Ras and H-Ras in Golgi membranes, RFP-tagged Ras proteins were co-expressed in COS-1 cells with each of the following GFP-tagged Golgi sub-compartment markers: GFP-KDELR (*cis* Golgi), mannosidase II-GFP (*medial* Golgi), or TGN 38/46-GFP (*trans* Golgi) (Supplemental Fig. 1B). GFP-tagged Ras proteins expressed in COS-1 cells have been previously shown to localize and become activated with a subcellular distribution comparable to that of endogenous Ras proteins (Chiu et al., 2002). Colocalization of Ras proteins and Golgi markers was assessed after 48 h of expression in at least 50 cells, scoring the colocalization for each image as low, moderate, or high based on the yellow pseudocolor generated by the confocal software for pixel colocalization in the Golgi area, as well as by overlapping morphologies of fluorescent structures.

This analysis showed that in more than 80% of the cells examined, RFP H-Ras colocalized to a high degree with markers of each of the three Golgi compartments (Fig. 1, and see Table I). In contrast, N-Ras was asymmetrically distributed within the Golgi cisterna, showing a high degree of colocalization (80% of the cells) with the KDEL-R marker of the *cis* compartment and mainly moderate or low colocalization (55% of the cells total) with the mannosidase II marker of the *medial* compartment. N-Ras showed the lowest degree of colocalization with the TGN 38/46 marker of the *trans* Golgi. It colocalized with this marker to a high degree in 32% of the cells examined and to a moderate or low degree in 68% of cells (Fig. 2 and see Table I). Thus, unlike H-Ras, N-Ras showed a polarized distribution in the Golgi, with enrichment in the *cis* Golgi compartment.

### The localization of N-Ras and H-Ras in Golgi membranes is determined by their different palmitoylation states

Because the association of the Ras isoforms with membranes depends, at least in part, on their acquisition of covalently linked palmitoyl groups, we examined the possibility that the degree of palmitoylation regulates the steady-state distribution of Ras in the Golgi apparatus. We therefore examined the distribution within the Golgi of Ras mutant proteins in which the number of palmitoyl residues in the two isoforms was reversed. RFP-H-Ras-Palm*N* designates an RFP-tagged H-Ras protein in which C184 is mutated to lysine, so that only the C181 residue was available as a site for palmitoylation, as is the case in wild-type N-ras (see Supplemental Fig. 1A). Conversely, a second palmitoylation site was introduced into N-Ras through mutation of leucine 184 to cysteine to yield the N-Ras-Palm*H* protein (see Supplemental Fig. 1A).

The pattern of Golgi membrane localization that was seen in confocal images for the singly palmitoylated H-Ras-Palm*N*

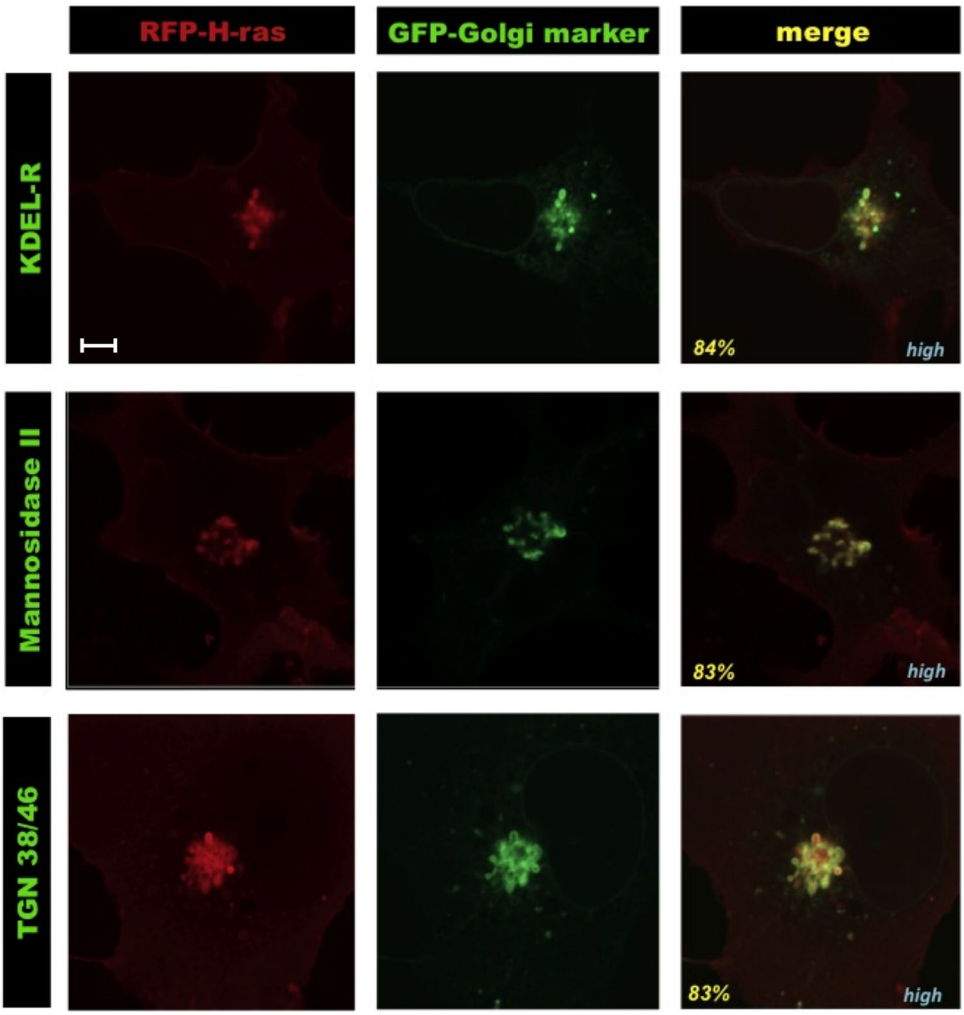


**Fig. 1. H-Ras has an even distribution pattern within the Golgi membrane of transfected COS-1 cells. Representative images of the localization pattern of RFP-H-Ras and the three GFP-tagged Golgi subcompartment markers. RFP-H-Ras is shown in the red channel of the images, the GFP-tagged Golgi subcompartment markers are shown in the green channel of the images, and the overlay of the red and green channels are also shown ("merge"). The text in the lower right corner of the third panel of each image (blue italics) indicates the overlap category that this particular imaged cell fell into, whereas the percentage values in the lower left corner (yellow italics) represents the percentage of cells that fell into this particular overlap category. Scale bar indicates 1 μm and applies to all images.**

mutant was very similar to that of singly palmitoylated, WT N-Ras. (Fig. 3A, and see Table I). Conversely, examination of images from COS cells expressing N-Ras-Palm*H* showed that the pattern of Golgi membrane localization of the doubly-palmitoylated N-Ras mutant protein was very similar to that of the wild type H-Ras. (Fig. 3B, and see Table I).

### Quantitative analysis of the distribution pattern of ras isoforms in Golgi membranes of transfected COS cells

Using the Zeiss ZEN software package (see Methods), we determined the degree of colocalization of each of the four RFP-tagged Ras isoforms with each of the GFP-tagged Golgi

TABLE I. Summary of the percentage of images examined that fell into the three overlap categories (H = high, M = moderate, and L = low overlap, respectively) for each of the twelve Ras and Golgi subcompartment marker transfection combinations

| | RFP-tagged Ras isoform | | | | | | | | | | | |
|---|---|---|---|---|---|---|---|---|---|---|---|---|
| | N-Ras | | | H-Ras-Palm*N* | | | H-Ras | | | N-RasPalm*H* | | |
| GFP-tagged Golgi marker | H | M | L | H | M | L | H | M | L | H | M | L |
| KDLER-R | 80 | 20 | — | 76 | 24 | — | 84 | 16 | — | 76 | 20 | 2 |
| Mannosidase II | 45 | 26 | 29 | 70 | 25 | 5 | 83 | 17 | — | 88 | 12 | — |
| TGN38/46 | 32 | 50 | 18 | 25 | 42 | 33 | 83 | 9 | 8 | 76 | 22 | 2 |
| | Singly palmitoylated | | | | | | Doubly palmitoylated | | | | | |

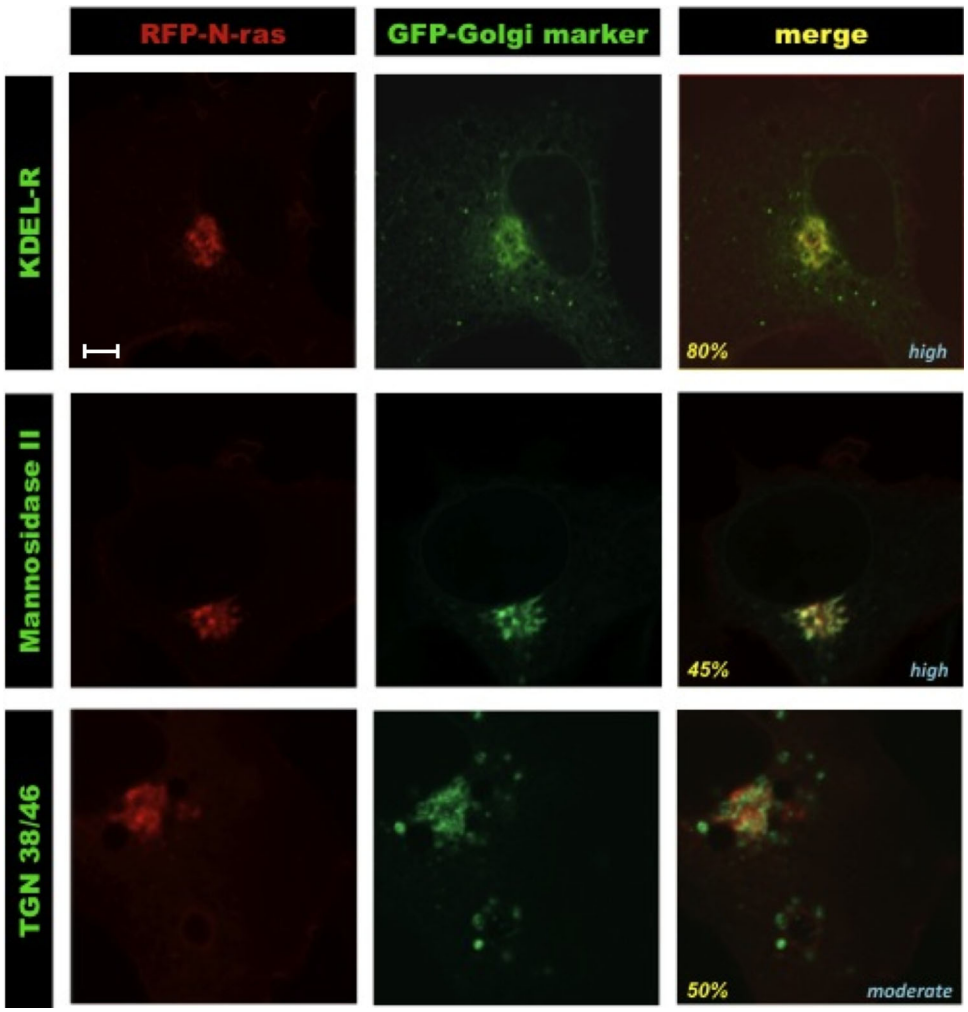


**Fig. 2. N-Ras has a polarized distribution pattern within the Golgi membrane of transfected COS-1 cells. (A) Representative images of the localization pattern of RFP-N-Ras and the three GFP-tagged Golgi subcompartment markers. RFP-N-Ras is shown in the red channel of the images, the GFP-tagged Golgi subcompartment markers are shown in the green channel of the images, and the overlay of the red and green channels are also shown ("merge"). The text in the lower right corner of the third panel of each image (blue italics) indicates the overlap category that this particular imaged cell fell into, whereas the percentage values in the lower left corner (yellow italics) represents the percentage of cells that fell into this particular overlap category. Scale bar indicates 1 μm and applies to all images.**

subcompartment markers in confocal images of transfected COS cells. The average Manders' overlap coefficient values obtained from this analysis are shown in Figure 4, for which the singly palmitoylated and doubly palmitoylated Ras isoforms, regardless of whether they were wild type or mutant, were treated as two different groups. The average Manders' and Pearson's coefficient values for the colocalization of the four individual Ras isoforms with the Golgi sub-compartment markers are shown in Supplemental Table 1.

The results of the quantitative analysis are in general agreement with the results of the qualitative analysis of the same confocal images. Both singly and doubly palmitoylated Ras isoforms had a high degree of overlap with the *cis* Golgi marker, KDEL-R, as evidenced by the high average Manders' coefficient values for both groups (0.8237 and 0.858, respectively—Fig. 4). In addition, the quantitative analysis revealed that the singly palmitoylated Ras isoforms had a much lower overlap (0.648) with the *trans* Golgi marker, TGN 38/46 than the doubly palmitoylated Ras isoforms (0.7832) ($P < 0.0001$—Fig. 4). The quantitative analysis also showed a high degree of colocalization of the singly and doubly palmitoylated Ras isoforms with the *medial* Golgi marker, mannosidase II (0.7813 and 0.82 average Manders' coefficient values, respectively—Fig. 4). Thus, the qualitative and quantitative analyses were in general agreement, in that both showed that doubly palmitoylated Ras isoforms had an even distribution pattern in Golgi membranes, whereas singly palmitoylated Ras isoforms had a polarized distribution pattern in the Golgi apparatus.

### Immuno-EM labeling experiments indicate that singly and doubly palmitoylated ras isoforms are differentially distributed across the golgi cisternal membranes

The distribution of epitope tagged H- and N-Ras isoforms and their palmitoylation mutants within stacks of Golgi cisternae was examined by immunogold-electron microscopy, in singly as well as in doubly transfected MDCK cells. This polarized epithelial cell line was chosen for the experiments because MDCK cells exhibit a very well developed and characterized

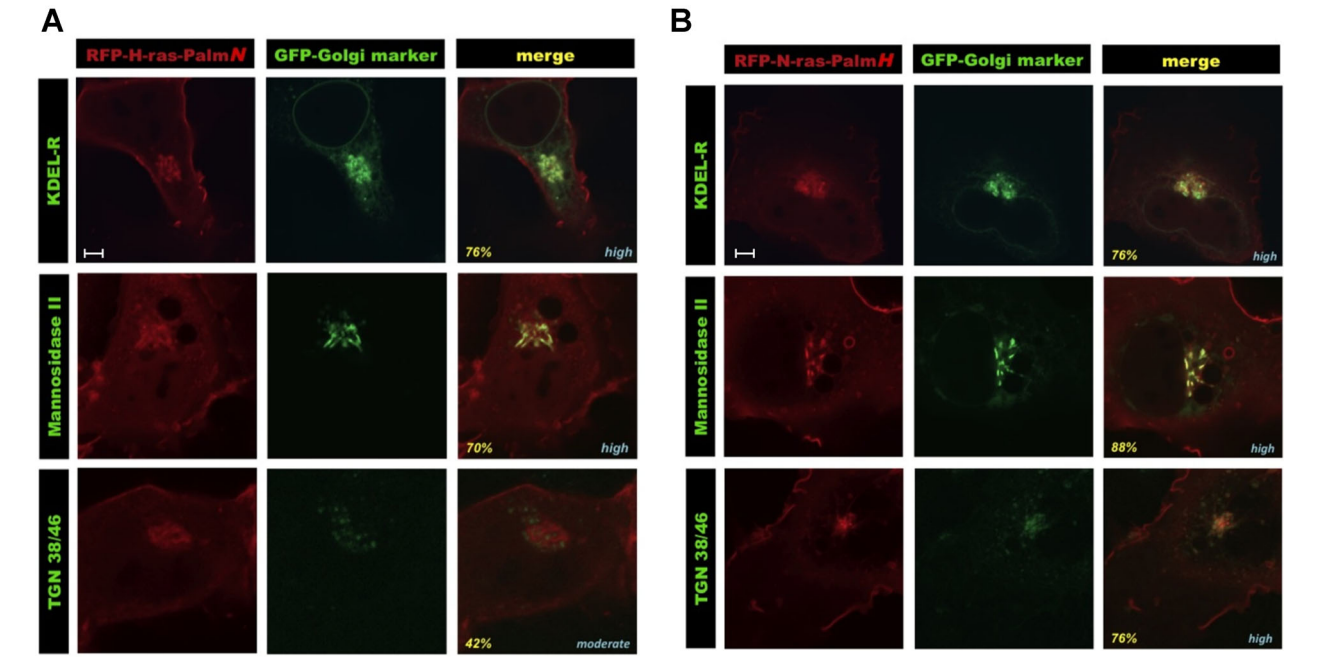


**Fig. 3. Doubly palmitolyated N-Ras-Palm*H* has an even distribution pattern within the Golgi membrane, whereas singly palmitoylated H-Ras-Palm*N* has a polarized distribution pattern. (A) Representative confocal images of COS-1 cells co-transfected with expression plasmids for RFP-N-ras-Palm*H* and either GFP-KDELR, Mannosidase II-GFP, or TGN38/46-GFP. RFP is shown in the first set of panels of each image; GFP is shown in the second set of panels; and the overlay of the red and green channels ("merge") is shown in the third set of panels of each image. The text in the lower right corner of the third panel of each image (blue italics) indicates the overlap category that this particular imaged cell fell into, whereas the percentage values in the lower left corner (yellow italics) represents the percentage of cells that fell into this particular overlap category. Scale bar indicates 1 μm and applies to all images in A. (B) Representative confocal images of COS-1 cells co-transfected with expression plasmids for RFP-H-ras-Palm*N* and either GFP-KDELR, mannosidase II-GFP, or TGN38/46-GFP. RFP is shown in the first set of panels of each image; GFP is shown in the second set of panels; and the overlay of the red and green channels ("merge") is shown in the third set of panels of each image. The text in the lower right corner of the third panel of each image (blue italics) indicates the overlap category that this particular imaged cell fell into, whereas the percentage values in the lower left corner (yellow italics) represents the percentage of cells that fell into this particular overlap category. Scale bar indicates 1 μm and applies to all images in B.**

Golgi apparatus that serves both apical and basolateral plasma membrane domains (Rindler et al., 1984). The cells were nucleofected with expression plasmids for either HA-tagged N-Ras, CFP-tagged H-Ras, CFP-tagged H-RasPalm*N*, or HA-tagged N-RasPalm*H*, and the labeled Ras isoforms were detected with anti-GFP or anti-HA antibodies, which were visualized with 6 or 10 nm protein A-conjugated gold particles. Figure 5 shows representative immuno-EM images obtained from MDCK cells that individually overexpressed one of the four tagged Ras proteins.

Overall, labeling for N-Ras was less intense than that for H-Ras, but distinct patterns of gold particle distribution were clear for both isoforms. In transverse sections of Golgi stacks, particles marking H-Ras were uniformly distributed throughout the cisternae (Fig. 5A), whereas those marking N-Ras had a polarized distribution towards one side of the cisternal Golgi stack (Fig. 5B). Because the immunofluorescence experiments showed that N-Ras colocalized strongly with KDEL-R and mannosidase II, we could ascertain that the highest concentration of N-Ras molecules was at the *cis*-most cisternae within the Golgi stack (Fig. 5A and B).

Parallel immuno-EM experiments with the mutant N-Ras-Palm*H* and H-RasPalm*N* proteins clearly confirm that singly palmitoylated H-Ras proteins acquired the polarized distribution characteristic of N-Ras, and that, conversely, double palmitoylation of N-Ras led to its broad distribution throughout the Golgi (Fig. 5C).

These results were confirmed with double labeling experiments. Differentially tagged Ras isoforms were coexpressed and were labeled by two different protocols, each employing a distinct antibody and gold particle size. Importantly, in some experiments the size of the gold particles used to mark each antibody was reversed to rule out the possibility that polarized labeling of the Golgi stacks was an artifact of the method. In the left panel (Fig. 6A), the larger 10 nm gold particles were used to label N-Ras and the smaller 6 nm particles to label H-Ras, whereas the reverse labeling was carried out for the right panel (Fig. 6B). Independently of the labeling protocol, doubly palmitoylated, wild type H-Ras molecules were present in cisternae throughout the Golgi stack, whereas singly palmitoylated N-Ras molecules revealed a polarized pattern.

## Discussion

Work from our laboratories and several others established the Golgi apparatus as the principal endomembrane compartment upon which N-Ras and H-Ras accumulate and signal (Choy and Philips, 2001; Chiu et al., 2002; Goodwin et al., 2005; Rocks et al., 2005). Recently, Misaki and colleagues (Misaki et al., 2010) challenged that view by suggesting that active Ras proteins instead localize predominantly to the recycling endosomes without expression on the Golgi. Our current results argue strongly for Golgi localization of N-Ras and H-Ras. Moreover, we did not observe a significant pool of these molecules

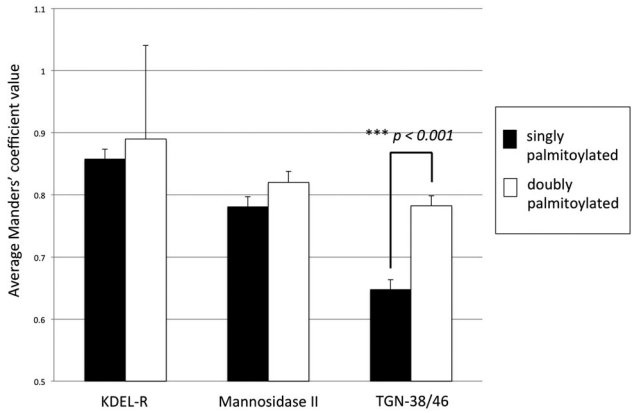


**Fig. 4. Quantitative analysis of images of transfected COS-1 cells supports the results of the qualitative image analysis. A comparison was made between the average Manders' coefficient colocalization values for either the RFP-tagged singly palmitolyated Ras isoforms (WT N-Ras and H-Ras-Palm*N*) or the RFP-tagged doubly palmitoylated Ras isoforms (WT H-Ras and N-Ras-Palm*H*) and each of the Golgi subcompartment markers (GFP-KDELR, Mannosidase II-GFP, and TGN38/46-GFP). Error bars indicate standard error of the mean. A Students' *t*-test revealed a statistically significant difference between the Manders' coefficient values of the singly and doubly palmitoylated Ras isoforms and TGN-38/46-GFP ($P < 0.001$).**

on endosomes with either live-cell confocal imaging or immunogold EM.

Our data also indicate that the distribution of N-Ras and H-Ras among the membrane stacks of the Golgi apparatus is dictated by the extent of palmitoylation of the proteins: whereas Ras proteins with two sites of palmitoylation are distributed homogeneously throughout the Golgi stacks, mono-palmitoylated Ras proteins are polarized toward the *cis* Golgi. What biochemical or biophysical properties or processes might account for this differential distribution?

To answer this question one must understand the processes through which Ras proteins become associated with membranes in general and Golgi membranes in particular. The fact that Ras proteins are synthesized on free polysomes and that farnesyltransferase is a soluble enzyme (Lane and Beese, 2006) indicates that Ras proteins begin their lives in the cytosol, where they are modified by a farnesyl lipid. The observations that mature Ras proteins are further modified by AAX proteolysis and carboxyl methylation and that the enzymes that catalyze these modifications, Rce1 and Icmt, are restricted to the ER (Dai et al., 1998; Schmidt et al., 1998) establishes that all Ras proteins must visit the cytosolic face of the ER, at least transiently. Because CAAX processing precedes palmitoylation (Ahearn et al., 2011b), one can deduce that Ras proteins visit the ER prior to their association with the Golgi. Thus, it is likely that nascent N-Ras and H-Ras gain access to the Golgi from the ER. Translocation from ER to Golgi could take place either via vesicular transport on the intermediates that carry secretory proteins or could occur via dissociation of Ras from the ER into the cytoplasmic fluid phase, followed by rebinding to membranes in the Golgi. The weak membrane affinity of proteins that are modified only with a farnesyl moiety (Silvius and l'Heureux, 1994), the existence of cytosolic chaperones capable of shielding the prenyl group of Ras proteins (Chandra et al., 2011), and the rapid recovery of GFP-Ras on the Golgi following photobleaching (Goodwin et al., 2005) all support the latter mechanism.

Complicating this scheme is the recent appreciation that the proportion of N-Ras or H-Ras that gains access to the Golgi does not consist of nascent proteins derived from the ER, but rather consists of depalmitoylated Ras molecules recycled from the PM to the Golgi via the cytosol. Indeed, as the half-life of Ras greatly exceeds that of its palmitoyl modification (Ahearn et al., 2011b), the bulk of the flux onto the Golgi likely derives from the PM.

The transport of secretory proteins from ER to Golgi via COPII-coated vesicles is tightly controlled in a vectorial manner by regulatory proteins, such as: the small GTPase Sar1 and the COPII subunits (Zanetti et al., 2012) that assure delivery only to the *cis* Golgi. Given the likely fluid phase delivery of depalmitoylated Ras to the Golgi, either as a nascent protein or as a protein recycled from the PM, the association with the Golgi via initial incorporation into the *cis* compartment is unlikely, as farnesylated non-palmitoylated Ras proteins should associate indiscriminately with all portions of the Golgi.

The driver of Ras association with Golgi membranes is thought to be the protein acyltransferase DHHC9/GPC16, as palmitoylation affords an "affinity trap" for Ras proteins with regard to membrane association. Accordingly, asymmetric distribution of DHHC9/GPC16 among Golgi cisternae could account for an asymmetric distribution of the palmitoylated products. Our finding that singly palmitoylated Ras molecules are concentrated in *cis* Golgi membranes, whereas doubly palmitoylated ones are found throughout the Golgi cisternae could be explained by a model in which the palmitoylating enzyme, DHHC9/GPC16, is enriched in the *cis* Golgi, where it would trap the soluble farnesylated Ras molecules in the membrane. Palmitoylated Ras proteins would then move by vesicular flow to the *medial* and *trans* Golgi compartments, and during this process, depalmitoylation would be expected to take place randomly. As they are transiting the Golgi, mono- palmitolyated Ras has a much higher probability of losing all acyl modifications and membrane affinity as a result of depalmitolyation than dipalmitolyated Ras, resulting in a paucity in the *trans* Golgi of molecules with a single palmitoylation site as compared to doubly palmitoylated ones. Unfortunately, reagents capable of reporting the localization of DHHC9/GPC16 within the Golgi have not yet been developed.

One problem with the model described above is that a paucity of palmitoylated N-Ras at the *trans* Golgi would make its delivery from the *trans* Golgi to the PM via vesicular transport much less efficient. One solution to this conundrum would be that mono-palmitoylated N-Ras takes an alternate path to the PM on vesicles that derive from the *cis* or *medial* Golgi. Such a pathway would be consistent with the recently proposed "rapid partitioning" model of Golgi trafficking (Patterson et al., 2008; Lippincott-Schwartz and Phair, 2010; Glick and Luini, 2011). The observation that some N-Ras containing, but not H-Ras containing, vesicles were occasionally seen adjacent to Golgi cisternae (data not shown) is consistent with the direct exit of mono-palmitoylated Ras isoforms from the *cis* or *medial* Golgi in vesicles destined for the PM rather than their emergence strictly from the TGN (Volchuk et al., 2000).

Any attempt to explain the differential distribution of N-Ras and H-Ras within the Golgi should take into account a possible role of the differential lipid composition of the various intracellular and plasma membranes. Whereas ER membranes are composed almost exclusively of glycerophospholipids and have little sphingolipids and cholesterol, the PM has a high concentration of these lipids that have a tendency to self assemble into liquid-ordered domains (Lippincott-Schwartz and Phair, 2010). Moreover, H-Ras has been localized to PM-associated microdomains or "nanoclusters," which are

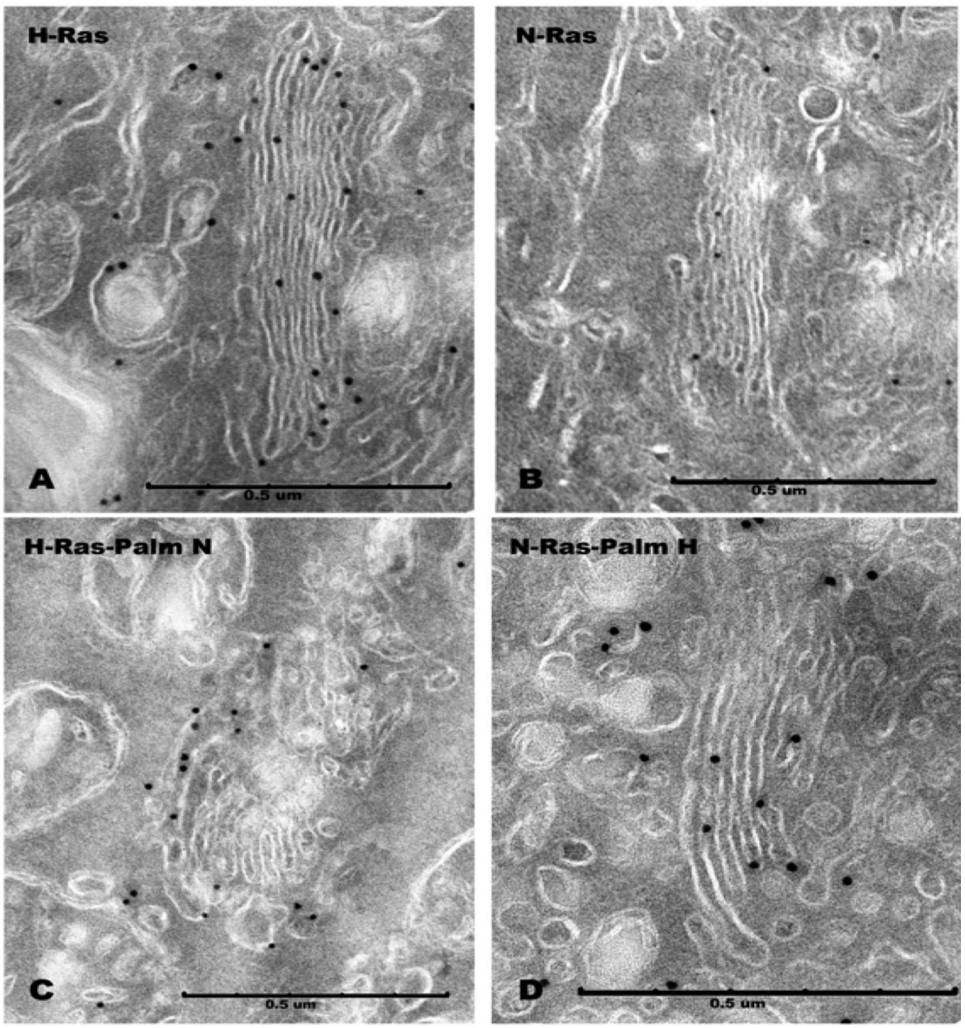


**Fig. 5. The differential distribution of H-Ras and N-Ras within the stack of cisternae in the Golgi apparatus is determined by their degree of palmitoylation. MDCK cells expressing the H- (A) or N-Ras (B) isoforms or their respective palmitoylation mutants (C and D) were processed for immuno electron microscopy with specific antibodies to: (A) CFP-tagged WT H-Ras. (B) HA-tagged WT N-Ras. (C) the CFP-tagged singly palmitoylated H-Ras-PalmN mutant. (D) the CFP-tagged doubly palmitoylated N-Ras-PalmH mutant. The antibodies were visualized with protein A-conjugated to 10 nm gold particles (see Materials and Methods).**

enriched in cholesterol and sphingolipids (Prior et al., 2001). Although the overall concentration of sphingolipids and cholesterol in the Golgi cisternae is relatively low, as proteins migrate distally through the Golgi stacks they encounter an increasing gradient of these lipids (Lippincott-Schwartz and Phair, 2010). Because saturated acyl chains favor partition into liquid-ordered domains, dipalmitoylated H-Ras is therefore more likely than monopalmitoylated N-Ras to partition into membranes with enrichment in sphingholipids and cholesterol, which could explain, at least in part, the difference we observed in their distribution across the Golgi stack.

Whatever the cause of the differential localization of N-Ras and H-Ras within the Golgi, this feature of Ras biology may have implications in signaling if relevant effectors are also asymmetrically distributed within the Golgi, especially as Golgi-localized Ras proteins have been previously shown to be able to signal from this organelle (Chiu et al., 2002). Consistent with this, our group has previously shown through mRNA expression profiling that N-Ras and H-Ras activate different downstream signaling programs in immune cells (Lynch SJ *et al.*, 2013). Overall, these results support the hypothesis that differential Ras isoform Golgi membrane localization translates to differential Golgi signaling.

## Materials and Methods

### Plasmid constructs

The RFP-N-Ras and RFP-H-Ras expression vectors used in the confocal studies were derived from pDsRed1-C1 (Clontech, Mountain View, CA), which produces a N-terminal fusion between the Ras protein and a monomeric form of RFP. The N-Ras-Palm*H* mutant contains a point mutation of L184 that converts it to a cysteine; N-Ras-Palm*H* therefore is doubly-palmitoylated, as is WT H-Ras (see Supplemental Fig. 1A). Similarly, the H-Ras-Palm*N* mutant has a mutation that converts C184 to a lysine; this mutant protein is singly-palmitoylated, as is WT N-Ras. The RFP-N-Ras-Palm*H* and the RFP-H-Ras-Palm*N* expression constructs were also derived from pDsRed1-C1. The GFP-KDELR construct had

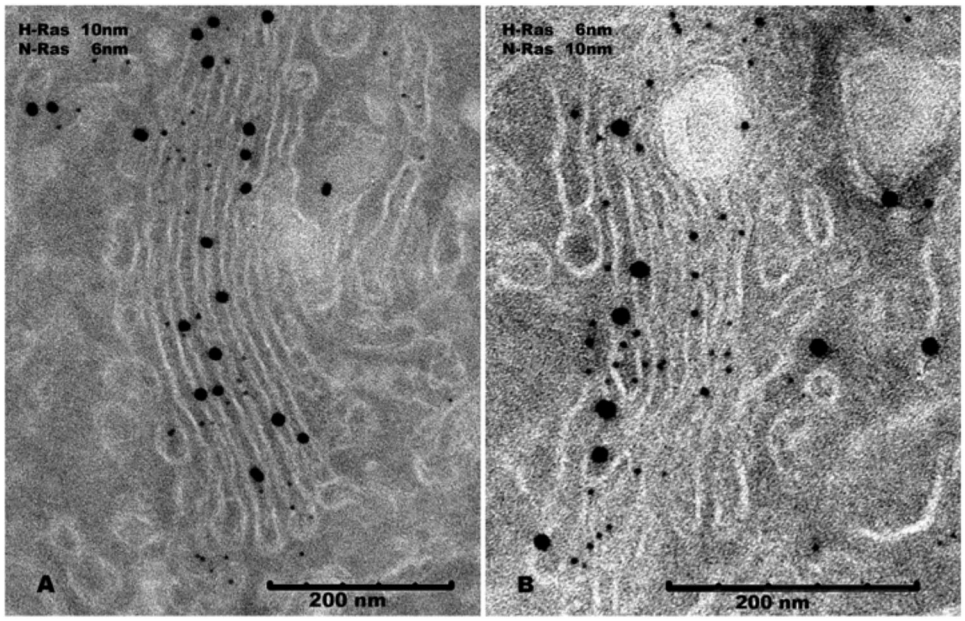


**Fig. 6. N-Ras and H-Ras molecules co-expressed in MDCK cells distribute differentially within the same Golgi stack. In the left panel (A) the larger (10 nm) gold particles were used to visualize the antibodies marking the GFP-tagged H-Ras, and the smaller (6 nm) particles to visualize the antibodies marking the HA-tagged N-Ras. The order in which the gold particles of different sizes was applied was reversed for the right panel (B). Although the polarized distribution of the 10 nm gold particles used to label N-Ras in Figure 6B is readily apparent, a close examination of the distribution of the smaller, 6 nm gold particles labeling N-Ras in Figure 6A reveals that these gold particles are preferentially localized to the first two-thirds of the Golgi cisternae and are not found in the distal third of the stack.**

been previously generated by Lippincott-Schwartz's group (Cole et al., 1998); this plasmid contained the D193N mutation, which greatly reduces retrograde transport of KDEL-R from the Golgi to the ER (Townsley et al., 1993). The Mannosidase II-GFP and TGN38/46-GFP expression constructs were gifts from Dr. Irma Sanchez (Department of Pathology—NYU Langone Medical Center). The TGN38/46-GFP expression plasmid we used was generated by Greer's group (Zirngibl et al., 2001).

The GFP-H-Ras expression vector used for immuno-EM experiments has been described elsewhere (Choy and Philips, 2001). The HA-N-Ras expression vector was a pCGN-based vector (Fiordalisi et al., 2001). The CFP-N-Ras, CFP-H-Ras, CFP-N-Ras-Palm*H*, and CFP-H-Ras-Palm*N* expression vectors were produced by cloning the human N-Ras, H-Ras, N-Ras- Palm*H*, and H-Ras-Palm*N* sequences into the multiple cloning site of the pECFP-C1 plasmid (Clontech). Plasmids for nucleofections were isolated from large-scale bacterial transformation cultures using an Endofree Plasmid Maxiprep Kit (Qiagen, Valencia, CA).

### Tissue culture

COS-1 cells were purchased from ATTC (Manassas, VA). The Madin-Darby canine kidney (MDCK) cell line was a gift from Dr. Jean-Pierre Simon (Department of Cell Biology—NYU Langone Medical Center); these cells were derived from a MDCK clone selected for the presence of particularly large and well-developed Golgi membranes (Simon J-P, personal communication). COS-1 cells were grown in DMEM (Mediatech, Corning, NY) supplemented with 10% FBS (Gibco, Grand Island, NY), 1% penicillin/streptomycin (Gibco, Grand Island, NY), and 0.1% normocin (Lonza, Allendale, NJ), whereas MDCK cells were grown in RPMI-1640 medium (Mediatech, Manassas, VA) supplemented with 10% FBS, 1% penicillin/streptomycin, and 0.1% normocin.

### Confocal live-cell imaging of transfected COS-1 cells

COS-1 cells were grown on 35 mm poly-L-lysine coated, glass bottom dishes (Mat Tek, Ashland, MA) to approximately 40% confluency, and were then transfected with Effectene reagent (Qiagen) according to a protocol from the manufacturer. The cells were co-transfected with 2 μg of the RFP-tagged Ras isoform expression construct and 2 μg of the GFP-tagged Golgi sub-compartment marker expression construct. Forty-eight hours post-transfection, the cells were visualized using a Zeiss 510 inverted confocal laser scanning microscope equipped with a 63 × 1.4 NA objective, with GFP excited with the 488 line of an argon laser and RFP excited with the 543 HeNe laser. For each of the individual co-transfections, the degree of overlap between the RFP-tagged Ras isoform and the GFP-tagged Golgi sub-compartment marker was assessed in at least 50 images. For each image, the extent of overlap was estimated to be within one of the following three categories: (1) high overlap, defined as: greater than 80% overlap between RFP and GFP, (2) moderate overlap, defined as: 40–80% overlap between RFP and GFP, and (3) low overlap, defined as: less than 40% overlap between RFP and GFP (see Supplemental Fig. 2 for examples of images for each overlap category). Then, for each co-transfection, the percentage of imaged cells with a degree of RFP:GFP overlap that fell into one of the three categories described above was determined.

### Quantitative analysis of confocal images

Confocal images were analyzed quantitatively for the extent of colocalization of RFP-tagged N- or H-Ras with each of the GFP-tagged Golgi sub-compartment marker proteins using the Zeiss ZEN software package. For each image, the quadrants of the

"scatter plot" produced by the ZEN software module were first adjusted to define any specific populations in the plot. Next, a region of interest (ROI) that corresponded to the Golgi was delineated, and finally, the Manders' and Pearson's overlap coefficients were computed for this ROI (see Supplemental Fig. 3), as well as for a region of similar size in the cytoplasm, but outside the Golgi area, from which background values were derived. The meaning and interpretation guidelines that we used for the Manders' and Pearson's colocalization coefficients are described in detail elsewhere (Zinchuk and Zinchuk, 2008). Only images with positive Pearson's coefficients were included in the quantitative analysis. For all of the images from each co-transfection, the individual Manders' and Pearson's coefficient values were averaged, and a standard error of the mean (SEM) was computed for each. An unpaired Student's *t*-test determined the statistical significance of differences of the averaged Manders' coefficients between experimental groups, where values of $P < 0.05$ were considered significant.

### Nucleofection of MDCK cells

For protein expression in MDCK cells, an Amaxa Biosystems Nucleofector II apparatus was used, in conjunction with the Amaxa Cell Line Nucleofector Kit L (Lonza). Nucleofections were performed according to the manufacturer's optimized protocol for MDCK cells. In brief: for each transfection, $8 \times 10^6$ trypsinized cells were processed for nucleofection with a total of 5 μg of plasmid DNA (either CFP or GFP-N-Ras, CFP or GFP-H-Ras, CFP-N-Ras-Palm*H* or CFP-H-Ras-Palm*N*) using the Amaxa nucleofector program A-024. We had previously found that MDCK cells that were plated at "super-confluency" (i.e., $2 \times 10^6$ cells/cm$^2$ or greater) develop large and clearly polarized stacks of Golgi cisterna. To achieve that density, pooled nucleofected MDCK cells were plated on 60 mm tissue culture plates. Unattached cells were removed after 24 h and at 48 h post-nucleofection attached cells were processed for immuno-EM labeling.

### Immuno-electron microscopy

Transfected cells in 60 mm dishes were fixed in 2% paraformaldehyde, 0.2% glutaraldehyde, for 2 h at room temperature. Cells were scraped off the dishes, and sedimented by centrifugation. Pellets were processed for cryosectioning, essentially as described elsewhere (Slot and Geuze, 2007). Frozen sections (70–80 nm in thickness) obtained in an ultramicrotome (Leica Ultracut, Buffalo Grove, IL), were picked up in 1.5% methylcellulose and 1.75% uranyl acetate (Liou et al., 1996). Aldehyde groups were quenched with glycine and the samples were incubated in 1% BSA to reduce background.

For single labeling with rabbit antibodies, sections were incubated with primary antibody overnight at 4°C and, after washing, incubated with protein A gold (10 nm) for 45 min at room temperature. Sections that were labeled with mouse or chicken primary antibody were then incubated with a bridge rabbit antibody, necessary for recognition by protein A gold. Following immunolabeling, the sections were fixed in 1% glutaraldehyde to stabilize the labeling.

For double labeling, after application and cross-linking of the first Ras-detecting specific antibody (rabbit, mouse, or chicken) and labeling with protein A gold (6 or 10 nm, using a bridge antibody if necessary), as described above, sections were once again washed, quenched, and blocked with BSA. Subsequently, the sections were incubated with the second Ras-detecting specific antibody, which was then labeled with protein A gold particles of a different size than those used for the first antibody.

After immunolabeling, sections were stained with neutral uranyl acetate and embedded in 1.8% methylcellulose before observation in a JEOL-1200 EXII electron microscope. In control experiments it was shown that omission of the first antibody eliminated the labeling with the corresponding gold particles and that omission of the second Ras-detecting specific antibody eliminated labeling by the second kind of protein A gold particles that were applied. This established that all the protein A binding antibodies used in the first round of labeling were saturated by the first type of protein A gold particles used and, therefore, were not available for binding to the second type of protein A gold particles.

### Antibodies used for immuno-EM

Chicken IgY anti-GFP was from Invitrogen (Carlsbad, CA), mouse monoclonal anti-HA from Covance (Madison, WI), rabbit monoclonal anti-HA from Cell Signalling (Danvers, MA), and rabbit anti-chicken and anti-mouse IgG and protein A gold was from EY Labs (San Mateo, CA).

## Acknowledgments

We would like to thank Dr. Irma Sanchez for providing the Mannosidase II-GFP and TGN38/46-GFP expression constructs. The Madin-Darby canine kidney (MDCK) cell line used for immuno-EM studies was a generous gift from Dr. Jean-Pierre Simon. We thank Martha Vega and Eleazar Vega Saenz de Miera for outstanding technical assistance.

## Literature Cited

Ahearn IM, Haigis K, Bar-Sagi D, Philips MR. 2011a. Regulating the regulator: post-translational modification of RAS. Nat Rev Mol Cell Biol 13:39–51.
Ahearn IM, Tsai FD, Court H, Zhou M, Jennings BC, Ahmed M, Fehrenbacher N, Linder ME, Philips MR. 2011b. FKBP12 binds to acylated H-ras and promotes depalmitoylation. Mol Cell 41:173–185.
Barbacid M. 1987. Ras genes. Annu Rev Biochem 56:779–827.
Bos JL. 1989. *Ras* oncogenes in human cancer: A review. Cancer Res 49:4682–4689.
Castellano E, Santos E. 2011. Functional specificity of Ras isoforms: So similar but so different. Genes Cancer 2:216–231.
Chandra A, Grecco HE, Pisupati V, Perera D, Cassidy L, Skoulidis F, Ismail SA, Hedberg C, Hanzal-Bayer M, Venkitaraman AR, Wittinghofer A, Bastiaens PI. 2011. The GDI-like solubilizing factor PDEδ sustains the spatial organization and signaling of Ras family proteins. Nat Cell Biol 14:148–158.
Chiu VK, Bivona T, Hach A, Sajous JB, Silletti J, Weiner H, Johnson RL, Cox AD, Philips MR. 2002. Ras signaling on the endoplasmic reticulum and the Golgi. Nature Cell Biol 4: 343–350.
Choy E, Philips M. 2001. Green fluorescent protein-tagged Ras proteins for intracellular localization. Methods Enzymol 332:50–64.
Cole NB, Ellenberg J, Song J, DiEuliis D, Lippincott-Schwartz J. 1998. Retrograde transport of Golgi-localized proteins to the ER. J Cell Biol 140:1–15.
Dai Q, Choy E, Chiu V, Romano J, Slivka S, Steitz S, Michaelis S, Philips MR. 1998. Mammalian prenylcysteine carboxyl methyltransferase is in the endoplasmic reticulum. J Biol Chem 273:15030–15034.
Dekker FJ, Rocks O, Vartak N, Menninger S, Hedberg C, Balamurugan R, Wetzel S, Renner S, Gerauer M, Scholemann B, Rusch M, Kramer JW, Rauh D, Coates GW, Brunsveld L, Bastiaens PI, Waldmann H. 2010. Small-molecule inhibition of APT1 affects Ras localization and signaling. Nat Chem Biol 6:449–456.
Esteban LM, Vicaro-Abejon C, Fernandez-Salguero P, Fernandez-Medarde A, Swaminathan N, Yienger K, Lopez E, Malumbres M, McKay R, Ward JM, Pellicer A, Santos E. 2001. Targeted genomic disruption of *H-ras* and *N-ras*, individually or in combination, reveals the dispensability of both loci for mouse growth and development. Mol Cell Biol 21: 1444–1452.
Farr CJ, Saiki RK, Erlich HA, McCormick F, Marshall CJ. 1988. Analysis of ras gene mutations in acute myeloid leukemia by polymerase chain reaction and oligonucleotide probes. Proc Natl Acad Sci USA 85:1629–1633.
Fiordalisi JJ, Johnson RL, 2nd, Ulku AS, Der CJ Cox. 2001. Mammalian expression vectors for Ras proteins: Generation and use of expression constructs to analyze Ras family function. Methods Enzymol 332:3–36.
Glick BS, Luini A. 2011. Membrane traffic within the Golgi apparatus. Cold Spring Harb Perspect Biol 3:a005215.doi: 10.1101/cshperspect.a005215.
Goodwin JS, Drake KD, Rogers C, Wright L, Lippincott-Schwartz J, Philips MR, Kenworthy AK. 2005. Depalmitolyated Ras traffics to and from the Golgi complex via a nonvesicular pathway. J Biol Chem 170:261–272.
Jannsen JWG, Steenvoorden ACM, Lyons J, Anger B, Bohlke JU, Bos JL, Seliger H, Bartram CR. 1987. *RAS* gene mutations in acute and chronic myelocytic leukemias. Proc Natl Acad Sci USA 84:9228–9232.
Koera K, Nakamura K, Nakao K, Miyoshi J, Toyoshima K, Hatta T, Otani H, Aiba A, Katsuki M. 1997. *K-ras* is essential for the development of the mouse embryo. Oncogene 15: 1151–1159.
Lane KT, Beese LS. 2006. Thematic review series: lipid posttranslational modifications. Structural biology of protein farnesyltransferase and geranylgeranyltransferase type I. J Lipid Res 47:681–699.
Leon J, Guerrero I, Pellicer A. 1987. Differential expression of the *ras* gene family in mice. Mol Cell Biol 7:1525–1540.
Liou W, Geuze HJ, Slot JW. 1996. Improving structural integrity of cryosections for immunogold labeling. Histochem Cell Biol 106:41–58.
Lippincott-Schwartz J, Phair RD. 2010. Lipid and cholesterol as regulators of traffic in the endomembrane system. Annu Rev Biophys 39:559–578.
Lorentzen A, Kinkhabwala A, Rocks O, Vartak N, Bastiaens PIH. 2010. Regulation of Ras localization by acylation enables a mode of intracellular propagation. Sci Signal 3:ra68.

Lynch SJ, Zavadil J, Pellicer A. 2013. In TCR-stimulated T- cells, N-ras regulates specific genes and signal transduction pathways. PLoS ONE 8:e63193.
Mangues R, Pellicer A. 1992. Ras activation in experimental carcinogenesis. Semin Cancer Biol 3:229–239.
Misaki R, Morimatsu M, Uemura T, Waguri S, Miyoshi E, Taniguchi N, Matsuda M, Taguchi T. 2010. Palmitoylated Ras proteins traffic through recycling endosomes to the plasma membrane during exocytosis. J Cell Biol 191:23–29.
Parikh C, Subrahmanyam R, Ren R. 2006. Oncogenic NRAS rapidly and efficiently induces CMML- and AML-like diseases in mice. Blood 108:2349–2357.
Parton RG, Hancock JF. 2004. Lipid rafts and plasma membrane microorganization: insights from Ras. Trends Cell Biol 14:141–147.
Patterson GH, Hirschberg K, Polishchuk RS, Gerlich D, Phair RD, Lippincott-Schwartz J. 2008. Transport through the Golgi apparatus by rapid partitioning within a two-phase membrane system. Cell 133:1055–1067.
Perez de Castro I, Bivona TG, Philips MR, Pelicer A. 2004. Ras activation in Jurkat cells following low-grade stimulation of the T-cell receptor is specific to N-ras and occurs only on the Golgi apparatus. Mol Cell Biol 24:3485–3496.
Perez de Castro I, Diaz R, Malumbres M, Hernandez MI, Jagirdar J, Jimenez M, Ahn D, Pellicer A. 2003. Mice deficient for N- *ras*: Impaired antiviral immune response and T-cell function. Cancer Res 63:1615–1622.
Plowman SJ, Hancock JF. 2005. Ras signaling from plasma membrane and endomembrane microdomains. Biochim Biophys Acta 1746:274–283.
Potenza N, Vecchione C, Notte A, De Rienzo A, Rosica A, Bauer L, Affuso A, De Felice M, Russo T, Poulet R, Cifelli G, De Vita G, Lembo G, Di Lauro R. 2005. Replacement of K-Ras with H-Ras supports normal embryonic development despite inducing cardiovascular pathology in adult mice. EMBO Rep 6:432–437.
Prior IA, Harding A, Yan J, Sluimer J, Parton RG, Hancock JF. 2001. GTP-dependent segregation of H-ras from lipid rafts is required for biological activity. Nat Cell Biol 3:368–375.
Rindler MJ, Ivanov IE, Plesken H, Rodriguez-Boulan E, Sabatini DD. 1984. Viral glycoproteins destined for apical and basolateral membrane domains traverse the same Golgi apparatus during their intracellular transport in doubly infected Madin–Darby canine kidney cells. J Cell Biol 98:1304–1319.
Rocks O, Peyker A, Kahms M, Verveer PJ, Koerner C, Lumbierres M, Kuhlmann HJ, Waldman H, Wittinghofer A, Bastiaens PIH. 2005. An acylation cycle regulates localization and activity of palmitoylated Ras isoforms. Science 307:1746–1752.
Roy S, Plowman S, Rotblat B, Prior IA, Muncke C, Grainger S, Parton RG, Henis YI, Kloog Y, Hancock JF. 2005. Individual palmitoyl residues serve distinct roles in H-ras trafficking, microlocalization and signaling. Mol Cell Biol 25:6722–6733.
Schmidt WK, Tam A, Fujimura-Kamada K, Michaelis S. 1998. Endoplasmic reticulum membrane localization of Rce1p and Ste24p, yeast proteases involved in carboxyl-terminal CAAX protein processing and amino-terminal a-factor cleavage. Proc Natl Acad Sci USA 95:11175–11180.
Silvius JR, l'Heureux F. 1994. Fluorimetric evaluation of the affinities of isoprenylated peptides for lipid bilayers. Biochem 33:3014–3022.
Slot JW, Geuze HJ. 2007. Cryosectioning and immunolabeling. Nat Protocols 10:2480–2491.
Swarthout JT, Lobo S, Farth L, Croke MR, Greentree WK, Deschenes RJ, Linder ME. 2005. DHHC9 and GCP16 constitute a human fatty acyltransferase with specificity for H- and N-Ras. J Biol Chem 280:31141–31148.
Townsley FM, Wilson DW, Pelham HR. 1993. Mutational analysis of the human KDEL receptor: distinct structural requirements for Golgi retention, ligand binding and retrograde transport. EMBO J 12:2821–2829.
Umanoff H, Edelmann W, Pellicer A, Kucherlapati R. 1995. The murine N-*ras* gene is not essential for growth and development. Proc Natl Acad Sci USA 92:1709–1713.
Volchuk A, Amherdt M, Ravazzola M, Brugger B, Rivera VM, Clarkson T, Perrelet A, Sollner TH, Rothman JE, Orci L. 2000. Megavesicles implicated in the rapid transport of intracisternal aggregates across the Golgi stack. Cell 102:335–348.
Zanetti G, Pahuja KB, Studer S, Shim S, Schekman R. 2012. COPII and the regulation of protein sorting in mammals. Nat Cell Biol 14:20–28.
Zinchuk V, Zinchuk O. 2008. Quantitative colocalization analysis of confocal fluorescence microscopy images. Curr Protoc Cell Biol 4.19.1–4.19.16.
Zirngibl R, Schulze D, Mirski SEL, Cole SPC, Greer PA. 2001. Subcellular localization analysis of the closely related Fps/Fes and Fer protein-tyrosine kinases suggests a distinct role for Fps/Fes in vesicular trafficking. Exper Cell Res 266:87–94.

## Supporting Information

Additional supporting information may be found in the online version of this article at the publisher's web-site.